Vacuum 202 (2022) 111141

Contents lists available at ScienceDirect

Vacuum

journal homepage: www.elsevier.com/locate/vacuum

Visualization of indentation induced sub-surface shear bands of Zr-based metallic glass by nanosecond pulse laser irradiation

Mingming Cui [a], Hu Huang [a,*], Chao Wang [a], Yongfeng Qian [a], Lin Zhang [b], Zhiyu Zhang [c], Jiwang Yan [b]

[a] Key Laboratory of CNC Equipment Reliability, Ministry of Education, School of Mechanical and Aerospace Engineering, Jilin University, Changchun, Jilin, 130022, China
[b] Department of Mechanical Engineering, Faculty of Science and Technology, Keio University, Yokohama, 223-8522, Japan
[c] State Key Laboratory of Nonlinear Mechanics, Institute of Mechanics, Chinese Academy of Sciences, Beijing, 100190, China

ARTICLE INFO

Keywords:
Metallic glass
Laser treatment
Nanoindentation
Shear band
Visualization

ABSTRACT

Characterizing the shear band of metallic glasses (MGs) is meaningful to understand its plastic deformation mechanism. However, the direct method for detecting the internal shear bands of deformed MGs with large field of view is still lacking. Inspired by the fact that surface defects have the enhanced absorption of laser energy, this study attempted to visualize the indentation induced sub-surface shear bands of Zr-based MG by nanosecond pulse laser irradiation in argon. The principle was first verified by laser irradiation of the surface scratch, and then implemented on the visualization of sub-surface shear bands. The experimental results demonstrated that the indentation induced sub-surface shear bands were successfully visualized by nanosecond pulse laser irradiation, and meanwhile, the laser irradiated surface maintained the amorphous characteristic. This study may open a new window for exploring the shear band characteristics of MGs upon external loads.

1. Introduction

Due to the absence of grain boundary and dislocation, metallic glasses (MGs) have excellent wear and corrosion resistance, high hardness and strength [1,2]. However, most of the MGs show quite poor plasticity at room temperature under tensile [3,4] or compression stress [5–8], which greatly restricts the application of MGs as structural and engineering materials. So, improving the plasticity of MGs has become one of the hot issues in the field of MGs, and currently, various methods have been proposed such as pre-deformation [9,10], introduction of elements [11–13], cryogenic cycling treatment [14,15], and ion irradiation [16]. Although these methods have effectively promoted the plasticity of MGs, the plastic deformation mechanism of MGs is still not clearly clarified. Shear bands are regarded as the main carrier of the plastic deformation of MGs, and the brittleness of MGs is closely related to the highly localized shear bands [17]. Therefore, a deeper understanding of shear bands is the key to developing MGs with good mechanical properties. Nevertheless, shear bands are small in size and complex in spatial distribution, making them difficult to observe, especially to detect the distribution and evolution of internal shear bands. Currently, the internal shear bands of deformed MGs are normally observed by the transmission electron microscope (TEM) [18,19]. However, due to its narrow field of view, TEM can only capture very limited local information of shear bands, far less than the complete information. X-ray and other detection methods can be used to reconstruct the image of internal shear bands in MGs [19–21], but these methods are not a direct way. Therefore, a more direct method with the ability of capturing large field of view is required to detect the internal shear bands of MGs. Inspired by the fact that surface defects have the enhanced absorption of laser energy [22,23], shear bands, as a kind of "defects" compared to the MG matrix, might be visualized by laser irradiation. Accordingly, to verify this idea, taking the indentation induced sub-surface shear bands of Zr-based MG as an example, we attempted to realize their visualization by nanosecond pulse laser irradiation. By tuning the peak laser power intensity, the indentation induced sub-surface shear bands were successfully visualized.

2. Materials and experiments

A typical Zr-based MG, $Zr_{41.2}Ti_{13.8}Cu_{12.5}Ni_{10}Be_{22.5}$ (at. %) was used

* Corresponding author.
E-mail address: huanghu@jlu.edu.cn (H. Huang).

https://doi.org/10.1016/j.vacuum.2022.111141
Received 14 April 2022; Received in revised form 1 May 2022; Accepted 3 May 2022
Available online 6 May 2022

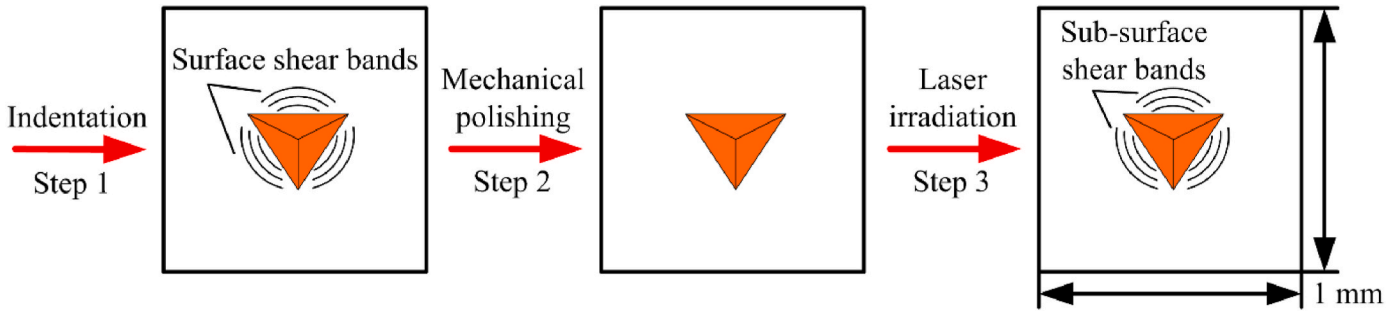

Fig. 1. The experimental procedures for the visualization of indentation induced sub-surface shear bands.

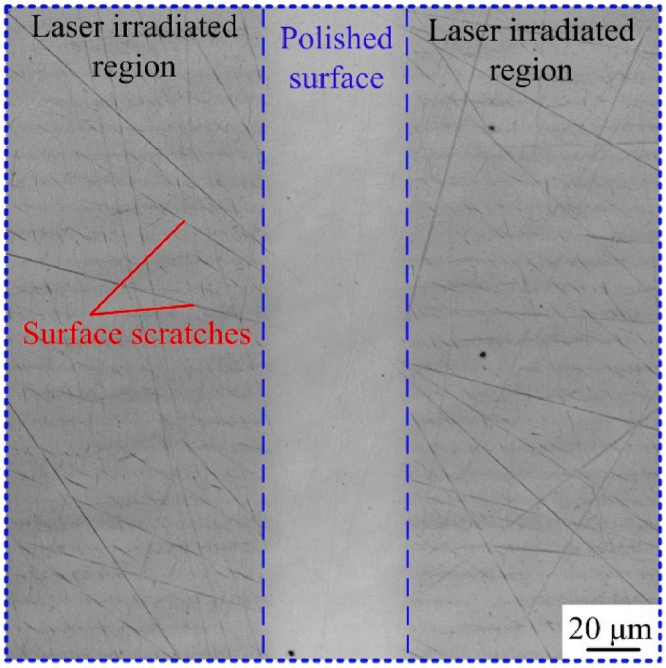

Fig. 2. Visualization of scratches on the polished surface by nanosecond pulse laser irradiation.

as the specimen in the experiments due to its high glass forming ability and commercial availability. The MG specimen was mechanically ground and then polished to achieve a mirror-like surface with a roughness around 10 nm. The scratch on the polished surface was a typical surface defect. To further demonstrate that the scratch as a surface defect had enhanced absorption of laser energy, the polished surface was irradiated by a nanosecond pulse laser (wavelength: 1064 nm, pulse width: 7 ns, repetition frequency: 800 kHz, spot diameter: ~43 μm) in argon atmosphere with pressure of 0.01 MPa. According to some pre-experiments, for visualization of the surface scratch, the employed peak laser power intensity, scanning speed and distance between two adjacent scanning lines were 8.7×10^{10} W/m^2, 5 mm/s and 10 μm, respectively.

To visualize the indentation induced sub-surface shear bands, the indentation experiments of Zr-based MG were performed first by using an indentation instrument (DUH-211s, SHIMADZU, Japan) with a pyramidal indenter. The loading rate was 50 mN/s and the indentation load was 1200 mN. By optical observation using the laser scanning digital microscope (LSDM, OLS4100, Olympus, Japan), the indentation induced surface shear bands were confirmed around the residual indents. Then, the sample was polished to remove these surface shear bands, which was confirmed by optical microscope observation. Finally, the sample was irradiated by the nanosecond pulse laser in argon. Fig. 1 illustrates the experimental procedures mentioned above. Similarly, by some pre-experiments, four peak laser power intensities, 8.3×10^{10} W/m^2, 8.7×10^{10} W/m^2, 9.0×10^{10} W/m^2 and 9.5×10^{10} W/m^2, were selected for the visualization of indentation induced sub-surface shear bands, and other experimental parameters were kept constant.

Morphologies of the residual indents after laser irradiation were observed by the LSDM. The amorphous characteristic of the MG was checked by an X-ray diffractometer (XRD, D8 Discover, Bruker, Germany) before and after laser irradiation.

3. Results and discussion

Fig. 2 shows the optical morphologies of the polished surface with two sides irradiated by the nanosecond laser. It is clearly seen that compared to the originally polished surface, the scratches on the laser irradiated regions become conspicuous, which confirms the fact that the scratch as a surface defect has the enhanced absorption of laser energy compared with the non-defect regions.

Inspired by the phenomenon shown in Fig. 2, the feasibility to visualize the indentation induced sub-surface shear bands by nanosecond laser irradiation was further explored. Figs. 3(a) and (c) present the residual indent (obtained under the indentation load of 1200 mN) before and after mechanical polishing. It is confirmed that after mechanical polishing, the indentation induced surface shear bands as well as the pile-up have been completely removed. By comparing the cross-sectional profiles illustrated in Figs. 3(b) and (d), it is noted that after mechanical polishing, the change in depth of the residual indent is quite small, and only a very thin layer is removed during the mechanical polishing.

The polished indents obtained under the load of 1200 mN were irradiated under various peak laser power intensities. Figs. 4(a)-(d) present the morphologies corresponding to the peak laser power intensities of 8.3×10^{10}, 8.7×10^{10}, 9.0×10^{10} and 9.5×10^{10} W/m^2, respectively. It is seen that the visualization of sub-surface shear bands is sensitive to the peak laser power intensity. When the peak laser power intensity is too low, the sub-surface shear bands would not be visualized as shown in Fig. 4(a); while, when the peak laser power intensity is too high, the ripples with a period of about 1 μm are observed on the MG surface, rather than sub-surface shear bands (see Fig. 4(b)). The

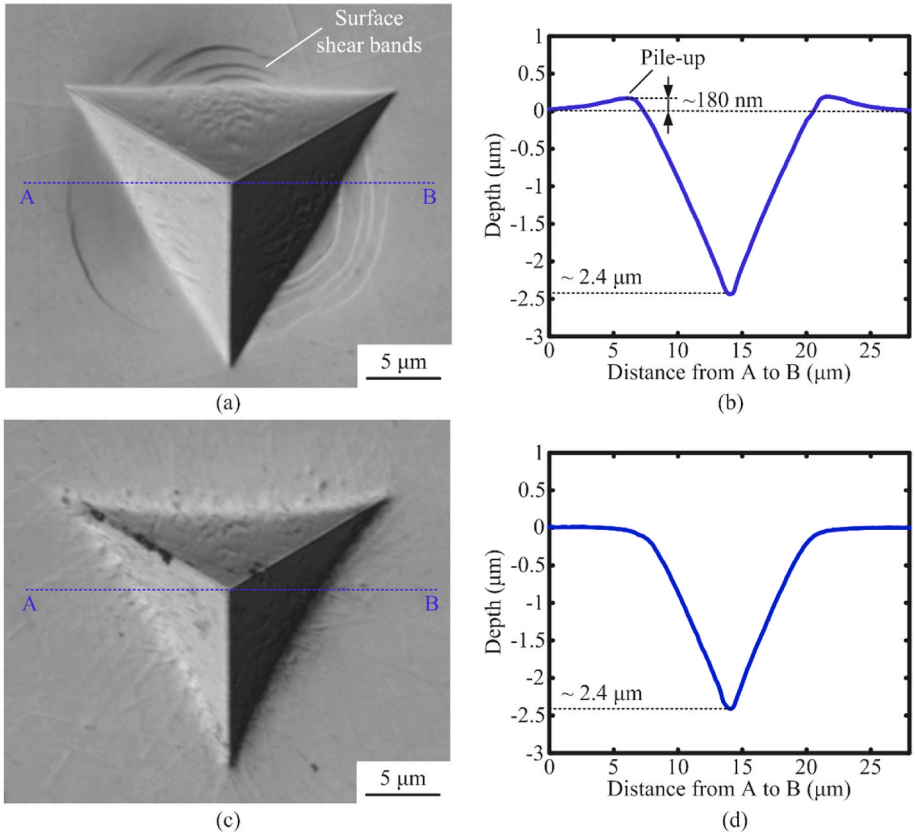

Fig. 3. The optical morphologies of the residual indent (obtained under 1200 mN): (a) before and (c) after mechanical polishing. (b) and (d) show the cross-sectional profiles of the dotted lines in (a) and (c), respectively.

formation of these ripples could be attributed to the interaction between the incident laser and excited molten surface waves, which has been elucidated in our previous study [24]. Nevertheless, as shown in Figs. 4 (b) and (c), under the peak laser power intensities of 8.7×10^{10} and 9.0×10^{10} W/m^2, the sub-surface shear bands have been successfully visualized. As mentioned in the introduction, surface defects such as scratches and micro-cracks, have the enhanced absorption of laser energy compared to the flat surface [22,23]. Compared to the MG matrix, the sub-surface shear bands here are regarded as a kind of "defects", and accordingly, more laser energy will be absorbed by them during the laser irradiation. This causes the sub-surface shear bands to be visible after laser irradiation. Moreover, by comparing Fig. 4(b) with its inset, it can be seen that the sub-surface shear bands almost reproduce the positions of the original surface shear bands, indicating that the laser irradiation does not change the spatial distribution of the shear bands.

To check whether laser irradiation has changed the amorphous characteristic of Zr-based MG, XRD is used to detect the polished surface and the surface irradiated under the peak laser power intensity of 9.5×10^{10} W/m^2, respectively. The results shown in Fig. 4(e) indicate that the MG maintains amorphous characteristic after laser irradiation.

4. Conclusion

In summary, being similar to the surface scratch, the indentation induced sub-surface shear bands of Zr-based MG showed different absorption characteristic of laser energy compared with the surrounded MG matrix, and thus they could be visualized by nanosecond pulse laser irradiation in argon. When the other laser parameters were fixed, the visualization of sub-surface shear bands was dependent on the peak laser power intensity. Furthermore, the visualization by nanosecond pulse laser irradiation did not change the amorphous characteristic of the MG. This study provides a direct method to visualize the internal shear bands of deformed MGs, which is meaningful to the research on shear band distribution and evolution.

CRediT authorship contribution statement

Mingming Cui: Writing – original draft, Visualization, Validation, Investigation, Formal analysis, Data curation. **Hu Huang:** Investigation, Methodology, Project administration, Resources, Supervision, Writing – review & editing, Funding acquisition, Conceptualization. **Chao Wang:** Investigation, Formal analysis, Data curation. **Yongfeng Qian:** Data curation, Investigation. **Lin Zhang:** Investigation, Data curation. **Zhiyu Zhang:** Data curation. **Jiwang Yan:** Supervision, Methodology.

Declaration of competing interest

The authors declare that they have no known competing financial interests or personal relationships that could have appeared to influence the work reported in this paper.

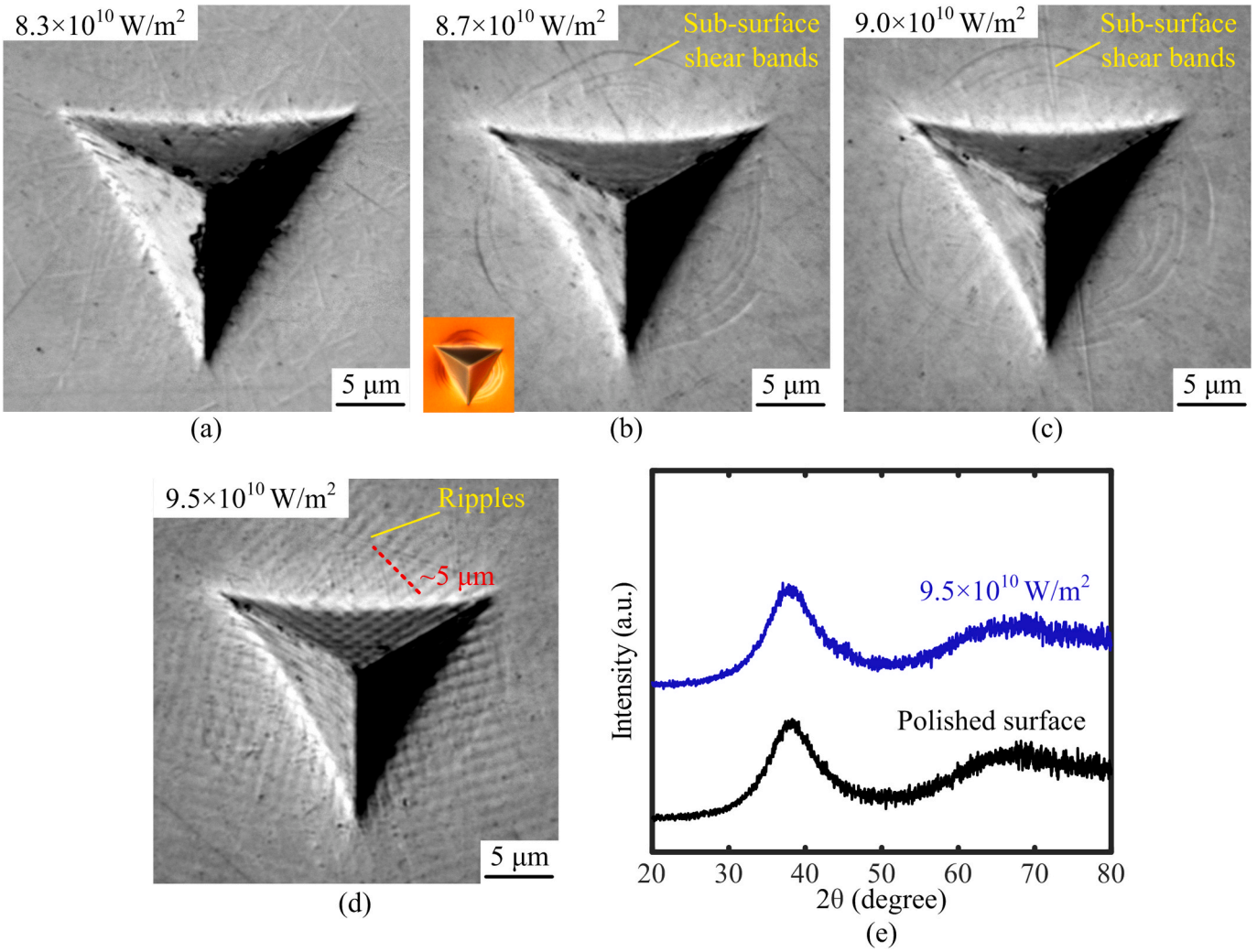

Fig. 4. The optical morphologies of the polished indents (obtained under 1200 mN) after laser irradiation under four peak laser power intensities: (a) 8.3×10^{10} W/m^2, (b) 8.7×10^{10} W/m^2, (c) 9.0×10^{10} W/m^2, and (d) 9.5×10^{10} W/m^2 (e) XRD patterns of the surface before and after laser irradiation. The inset of Fig. 4(b) shows the optical morphology of the original residual indent corresponding to Fig. 4(b).

Acknowledgements

This work was supported by the National Natural Science Foundation of China (Grant No. 51705197), the Graduate Innovation Fund of Jilin University (Grant No. 101832020CX106), and the Fundamental Research Funds for the Central Universities (2019–2022).

References

[1] Q. Halim, N.A.N. Mohamed, M.R.M. Rejab, W.N.W.A. Naim, Q. Ma, Metallic glass properties, processing method and development perspective: a review, Int. J. Adv. Manuf. Technol. 112 (5) (2021) 1231–1258.
[2] G. Huang, L. Qu, Y. Lu, Y. Wang, H. Li, Z. Qin, X. Lu, Corrosion resistance improvement of 45 steel by Fe-based amorphous coating, Vacuum 153 (2018) 39–42.
[3] T. Wang, Q. Hou, L. Zhang, Enhanced heterogeneity and plasticity in a Zr-Cu-Al bulk metallic glass with micro-addition of oxygen, Mater. Sci. Eng., A 831 (2022), 142222.
[4] R. Qu, R. Maaß, Z. Liu, D. Tönnies, L. Tian, R.O. Ritchie, Z. Zhang, C.A. Volkert, Flaw-insensitive fracture of a micrometer-sized brittle metallic glass, Acta Mater. 218 (2021), 117219.
[5] Z. Chu, B. Huang, G. Yuan, J. Zhang, J. Yin, W. Ding, Microstructure and fracture behavior of $Zr_{55}Cu_{30}Al_{10}Ni_5$ bulk metallic glass and its composites containing ZrO_2, Rare Met. Mater. Eng. 40 (5) (2011) 765–768.
[6] A.Y. Churyumov, A.I. Bazlov, A.A. Tsarkov, A.N. Solonin, D.V. Louzguine-Luzgin, Microstructure, mechanical properties, and crystallization behavior of Zr-based bulk metallic glasses prepared under a low vacuum, J. Alloys Compd. 654 (2016) 87–94.
[7] F. Farahani, R. Gholamipour, Giant size effect on compressive plasticity of $(Zr_{55}Cu_{30}Al_{10}Ni_5)_{99}Nb_1$ bulk metallic glass, Mater. Sci. Eng., A 651 (2016) 968–975.
[8] F. Farahani, R. Gholamipour, Statistical weibull analysis of compressive fracture strength of $(Zr_{55}Cu_{30}Al_{10}Ni_5)_{99}Nb_1$ bulk metallic glass, J. Alloys Compd. 695 (2017) 2740–2744.
[9] X.H. Sun, Y.S. Wang, J. Fan, H.J. Yang, S.G. Ma, Z.H. Wang, J.W. Qiao, Plasticity improvement for dendrite/metallic glass matrix composites by pre-deformation, Mater. Des. 86 (2015) 266–271.
[10] P. Zhang, C. Zhang, D. Ouyang, L. Liu, Enhancement of plasticity and toughness of 3D printed binary $Zr_{50}Cu_{50}$ bulk metallic glass composite by deformation-induced martensitic transformation, Scripta Mater. 192 (2021) 7–12.
[11] S. Chen, J. Wu, J. Tu, X. Li, J. Zou, Q. Hu, X. Zeng, Enhanced plasticity in a Ti-Ni-Nb-Zr shape memory bulk metallic glass composite with high Nb addition, Mater. Sci. Eng., A 704 (2017) 192–198.
[12] W.H. Zhou, F.H. Duan, Y.H. Meng, C.C. Zheng, H.M. Chen, A.G. Huang, Y.X. Wang, Y. Li, Effect of alloying oxygen on the microstructure and mechanical properties of Zr-based bulk metallic glass, Acta Mater. 220 (2021), 117345.
[13] G. Widjaja, K. Ershov, S. Chupradit, W. Suksatan, M. Kavitha, M.A. Jawad, I. Fardeeva, S.T. Ghafel, Y.F. Mustafa, M.M. Kadhim, S. Sajjadifar, The effects of hydrogen doping on energy state of shear bands in a Zr-Based metallic glass, Vacuum 198 (2022), 110882.
[14] Y. Du, W. Han, Q. Zhou, Y. Xu, H. Zhai, V. Bhardwaj, H. Wang, Enhancing the plasticity of a Ti-based bulk metallic glass composite by cryogenic cycling treatments, J. Alloys Compd. 835 (2020), 155247.
[15] S. Di, Q. Wang, J. Zhou, Y. Shen, J. Li, M. Zhu, K. Yin, Q. Zeng, L. Sun, B. Shen, Enhancement of plasticity for FeCoBSiNb bulk metallic glass with superhigh strength through cryogenic thermal cycling, Scripta Mater. 187 (2020) 13–18.
[16] P. Xue, S. Pauly, W. Gan, S. Jiang, H. Fan, Z. Ning, Y. Huang, J. Sun, Enhanced tensile plasticity of a CuZr-based bulk metallic glass composite induced by ion irradiation, J. Mater. Sci. Technol. 35 (10) (2019) 2221–2226.

[17] G.H. Duan, M.Q. Jiang, X.F. Liu, L.H. Dai, J.X. Li, In-situ observations on shear-banding process during tension of a Zr-based bulk metallic glass composite with dendrites, J. Non-Cryst. Solids 565 (2021), 120841.
[18] C. Liu, V. Roddatis, P. Kenesei, R. Maaß, Shear-band thickness and shear-band cavities in a Zr-based metallic glass, Acta Mater. 140 (2017) 206–216.
[19] C. Liu, Z. Cai, X. Xia, V. Roddatis, R. Yuan, J.M. Zuo, R. Maaß, Shear-band structure and chemistry in a Zr-based metallic glass probed with nano-beam x-ray fluorescence and transmission electron microscopy, Scripta Mater. 169 (2019) 23–27.
[20] C. Liu, A. Das, W. Wang, S. Küchemann, P. Kenesei, R. Maaß, Shear-band cavities and strain hardening in a metallic glass revealed with phase-contrast x-ray tomography, Scripta Mater. 170 (2019) 29–33.
[21] Y. Mo, X. Tang, L. Meng, J. Qiao, X. Yao, Spatial–Temporal evolution of shear banding in bulk metallic glasses, Mater. Sci. Eng., A 800 (2021), 140286.
[22] H. Huang, J. Yan, Surface patterning of Zr-based metallic glass by laser irradiation induced selective thermoplastic extrusion in nitrogen gas, J. Micromech. Microeng. 27 (7) (2017), 075007.
[23] H. Huang, Y.F. Qian, C. Wang, J.W. Yan, Laser induced micro-cracking of Zr-based metallic glass using 10^{11} W/m^2 nano-pulses, Mater. Today Commun. 25 (2020), 101554.
[24] Y. Qian, H. Huang, C. Wang, P. Yu, J. Xu, Z. Zhang, Formation of leaf-shaped microstructure on Zr-based metallic glass via nanosecond pulsed laser irradiation, J. Manuf. Process. 72 (2021) 61–70.